Muon Spin Relaxation Study of the Magnetism in Unilluminated Prussian Blue Analogue Photo-magnets

Z. Salman,[1] T.J. Parolin,[2] K.H. Chow,[3] T.A. Keeler,[4] R.I. Miller,[1] D. Wang,[4] and W.A. MacFarlane[2]

[1] *TRIUMF, 4004 Wesbrook Mall, Vancouver, BC, Canada, V6T 2A3*
[2] *Chemistry Department, University of British Columbia, Vancouver, BC, Canada V6T 1Z1*
[3] *Department of Physics, University of Alberta, Edmonton, AB, Canada T6G 2J1*
[4] *Department of Physics and Astronomy, University of British Columbia, Vancouver, BC, Canada V6T 1Z1*

We present longitudinal field muon spin relaxation (μSR) measurements in the unilluminated state of the photo-sensitive molecular magnetic Co-Fe Prussian blue analogues $M_{1-2x}Co_{1+x}[Fe(CN)_6]\cdot zH_2O$, where M=K and Rb with $x = 0.4$ and $\simeq 0.17$, respectively. These results are compared to those obtained in the $x = 0.5$ stoichiometric limit, $Co_{1.5}[Fe(CN)_6]\cdot 6\ H_2O$, which is not photo-sensitive. We find evidence for correlation between the range of magnetic ordering and the value of x in the unilluminated state which can be explained using a site percolation model.

A. Introduction

Prussian Blue (PB) ($Fe_4[Fe(CN)_6]_3$) is a long-known dye and prototypical transition metal co-ordination compound that exhibits ferro-magnetism [1, 2, 3] driven by superexchange coupling between iron spins. It is an important case of exchange coupling mediated through the CN^- bridge [4]. Much of the recent interest in magnetic compounds related to PB (including a few that have been studied with μSR [5, 6, 7]) is motivated by potential novel behavior and related applications in molecular magnetism [8, 9], including magnetism that is sensitive to exposure to light, i.e. *photomagnetism*.

The compounds studied in this paper are the molecule based Co-Fe PB analogues (Co-Fe PBAs) $M_{1-2x}Co_{1+x}[Fe(CN)_6]\cdot zH_2O$[1] (M is an alkali metal) [8, 9, 12]. These compounds have the sodium chloride structure, with Co and Fe ions located on the vertices of a cubic lattice, each octahedrally coordinated by six cyano moieties (Fig. 1). The Co and Fe ions are connected via cyanide bridges with interstitial alkali metal ions and water molecules [9, 13] (Fig. 1(b)). Co-Fe PBAs are in general non-stoichiometric and significant structural disorder (vacancies in the $Fe(CN)_6$ sites) is present. Depending on the stoichiometry and synthesis route, the materials are paramagnets or exhibit magnetic ordering at temperatures below $\sim$ 25 K, due to small superexchange coupling J between Fe^{III} and Co^{II} moments.

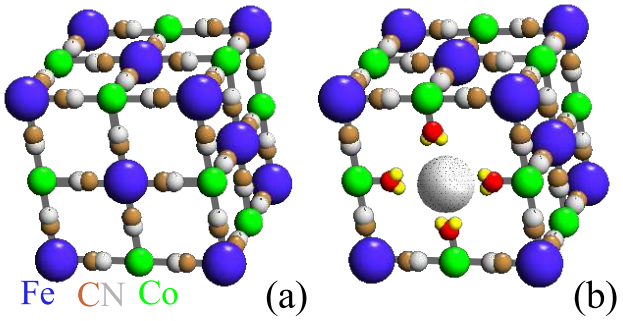

FIG. 1: (Color online) Crystal structure of $M_{1-2x}Co_{1+x}[Fe(CN)]\cdot zH_2O$: (a) $x = 0.5$; (b) $x \neq 0.5$, with an $Fe(CN)_6$ vacancy shown in gray coordinated by bound water molecules. Large, medium and small circles denote Fe, Co, and CN, respectively. The alkali ions which maintain charge neutrality occupy cubic interstitial sites (not shown).

Illumination of Co-Fe PBAs with broadband visible light in the range of $\sim 550 - 750$ nm can cause dramatic changes in the magnetic properties, including an increase in magnetization and ordering temperature. The proposed origin of the photomagnetic effect is a light-induced charge transfer from the state: $Fe^{II}(t_{2g}^6, S = 0)$-CN-$Co^{III}(t_{2g}^6, S = 0)$ to the meta-stable self–trapped state: $Fe^{III}(t_{2g}^5, S = 1/2)$-CN-$Co^{II}(t_{2g}^5 e_g^2, S = 3/2)$ [9, 14], effectively increasing the concentration of magnetic moments. The non-stoichiometry is believed essential for the photoinduced magnetization [14]. However, in spite of considerable experimental and theoretical effort, the microscopic mechanism of the photomagnetic effect and the nature of magnetic ordering remain unclear, often because conclusions are drawn solely on the basis of macroscopic magnetization measurements [12].

In this paper we present the results of muon spin relaxation (μSR) studies in three related Co-Fe PBA compounds: $Co_{1.5}[Fe(CN)_6]\cdot 6H_2O$ which is the stoichiometric limit $x = 0.5$, as well as $K_{0.2}Co_{1.4}[Fe(CN)_6]\cdot 6.9H_2O$ and $Rb_{0.66}Co_{1.25}[Fe(CN)_6]\cdot 4.3H_2O$. For clarity, we abbreviate these henceforth as $Co_{1.5}$, $K_{0.2}Co_{1.4}$ and $Rb_{0.66}Co_{1.25}$ respectively. Both $K_{0.2}Co_{1.4}$ and $Rb_{0.66}Co_{1.25}$ exhibit photomagnetism. In particular, $K_{0.2}Co_{1.4}$ shows an enhancement of its ferrimagnetic

[1] This chemical formula is a commonly used approximation though the ratio M:Co may be slightly different [10, 11].

transition temperature and magnetization [9, 17], while $Rb_{0.66}Co_{1.25}$ shows a transition from paramagnetic to ferrimagnetic behavior [13]. The results presented here deal with the unilluminated state these materials, i.e. in absence of light. We find that even in this state there is some degree of magnetic ordering, depending on the concentration of vacancies. In both $Co_{1.5}$ and $K_{0.2}Co_{1.4}$ we find evidence for static magnetic order. In contrast, the moments remain dynamic in $Rb_{0.66}Co_{1.25}$, but there is clear indication of magnetic cluster formation. These results are consistent with a site percolation model [15], where long range order is achieved when the concentration of magnetic centers (Fe^{III} and Co^{II}) is above a 3D critical value $p_c = 0.3116$ [15, 16].

B. Experimental

The three Co-Fe PBA compounds were obtained by aqueous precipitation followed by high speed centrifugation and drying, and consist of very fine (sub-micron sized) powders. Several hundred mg of each material was used in the μSR experiments. The samples were placed on a transparent Lucite sample holder and mounted in a horizontal helium gas flow cryostat with a bore of about 5 cm coaxial with the muon beam. Surface muons (4.1 MeV) entered the cryostat via thin Kapton windows. The range of surface muons is about 120 mg/cm^2 (which is somewhat reduced by the intervening Kapton windows and thin muon counter). This means that for materials of typical solid densities, the muons penetrates on the order of 100 μm. In addition, the amount of sample used in our measurements was more than $\sim$ 200 mg/cm^2 to prevent muons from penetrating through the sample.

The μSR experiments were performed on the M20 beamline at TRIUMF, where 100% spin polarized positive muons (gyromagnetic ratio $\gamma = 13.55$ MHz/kG) are implanted into the sample. The time evolution of the muon spin polarization depends on the distribution of internal magnetic fields and their temporal fluctuations. The implanted muons decay (β^+ decay with lifetime $\tau = 2.2$ μs) emitting a positron preferentially along the direction of the muon spin at the time of decay. The muon spin polarization as a function of time is thus proportional to the asymmetry of β decay along the initial spin direction. In magnetic materials, the unpaired spins fluctuate rapidly in the paramagnetic state, but as the transition temperature is approached upon cooling, the critical slowing down of the electronic moments brings the magnetic fluctuations into a time range where they cause the muon spin to relax. In the ordered state, the moments yield a static internal magnetic field which affects the precession of the muon spin. An extensive review of μSR in magnetic materials is given in Ref. [18]. Further details on the μSR technique may be found in Refs. [19, 20, 21, 22].

For the optical excitation experiments, light was introduced from the downstream end of the cryostat, with the light source approximately 1 m from the sample. The white light intensity from the tungsten-halogen source used was estimated to be at least 50 mW/cm^2 at the sample, and we used both white and red filtered light using low pass colored glass (RG665 or OG590) filters from Melles-Griot. Initially light was introduced via a UVT Lucite lightguide, but due to concern over IR absorption, this was modified, first to a $\sim$ 6 mm thick Lucite window, then to an IR transparent Pyrex window. The optical transmission for visible light, in both UVT Lucite (all thicknesses) and Pyrex (5 mm thick window), is better than 90%, ensuring that the samples are illuminated with sufficient intensity in the range $\sim 550 - 750$ nm. In these experiments the samples were illuminated from the back through the transparent sample holder and/or from the front (facing the muon beam) using a spherical mirror with an on-axis aperture to allow the muon beam to arrive at the sample.

C. Results in $Co_{1.5}$: the Stoichiometric Limit $x = 0.5$

The compound $Co_{1.5}$ was prepared following the procedure described in Ref.[13]. The color, temperature and field dependencies of the magnetization and the infrared (IR) frequencies of the CN stretch modes are in agreement with previous work [13]. The magnetization (M) was measured as a function of temperature using a SQUID magnetometer (see Fig. 2). Upon zero field cooling (ZFC), M increases dramatically at $T_c \sim 15$ K and decreases when cooled further; similarly, the field cooled (FC) magnetization exhibits an increase at T_c then saturates at low temperatures. Earlier studies [13] indicate

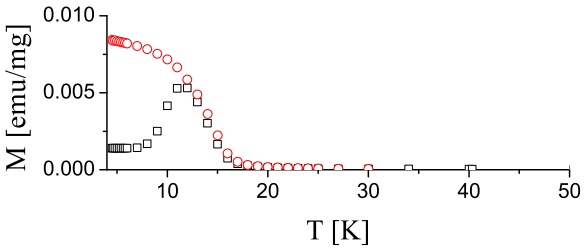

FIG. 2: The zero field (squares) and field (circles) cooled DC magnetization of $Co_{1.5}$ measured at 100 G in a SQUID magnetometer.

that the $Co_{1.5}$ compound becomes ferrimagnetic at T_c in agreement with our measurements.

The longitudinal field (LF) μSR measurements in $Co_{1.5}$ give information on the behavior of muons in the PBAs structure with dense Fe^{III} and Co^{II} moments, which serve as a point of comparison for the other materials studied in this work. Fig. 3 shows an example of the muon spin relaxation spectra for different tempera-

tures. Note the asymmetry below 12.5 K exhibits a dip at early times $t \sim 0.05$ μs (Fig. 3(a)), but then recovers to a higher value at longer times and continues relaxing slowly down to zero (Fig. 3(b)). This type of muon spin relaxation is a clear indication of a broad distribution of *static* local fields at the muon site [23]. When the

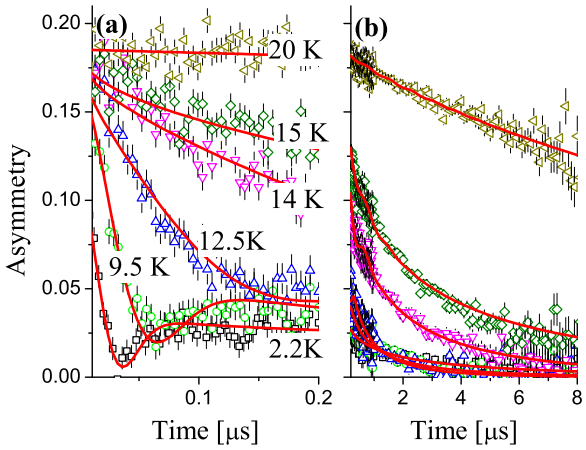

FIG. 3: (Color online) The muon spin relaxation as a function of time measured in $Co_{1.5}$ at 100 G longitudinal field for different temperatures at (a) early and (b) long times. The solid lines are fits to the function described in the text.

muon experiences a distribution of static magnetic fields $\rho\left(\frac{\gamma^2(\mathbf{B}-\mathbf{B}_s)^2}{\Delta^2}\right)$, where $\mathbf{B}_s$ is the average static field and Δ is the root mean square of the field distribution, the asymmetry follows a static Kubo-Toyabe function

$$\begin{aligned} A_{\rm KT}(t) &= A_0 \int \rho\left(\frac{\gamma^2(\mathbf{B}-\mathbf{B}_s)^2}{\Delta^2}\right) G_z(t) d^3B \\ G_z(t) &= Re\left\{\cos^2\theta + \sin^2\theta e^{i\gamma Bt}\right\} \end{aligned} \quad (1)$$

where θ is the angle between the initial muon spin and the local static magnetic field $\mathbf{B}$ which is averaged over a powder sample. For example, if $\mathbf{B}_s = 0$ then the asymmetry is at its maximum value at $t = 0$, it exhibits a dip at $t \sim 1/\Delta$ and recovers to $\sim 1/3$ its initial value at long times. Depending on the form of the field distribution, e.g. Gaussian or Lorentzian, the relaxation follows a Gaussian Kubo-Toyabe (GKT), $A_{\rm GKT}$, or a Lorentzian Kubo-Toyabe (LKT), $A_{\rm LKT}$, respectively. However, if in addition to the static field component a small fluctuating field $B_d(t)$ is present, then the 1/3 tail continue to relax to zero [23]. The relaxation can be described by a phenomenological function: a LKT or GKT multiplied by a suitable dynamic relaxation function. The asymmetry in Fig. 3 was found to fit best to GKT multiplied by a square root exponential relaxation,

$$A(t) = A_{\rm GKT}(t) e^{-\sqrt{\lambda t}}. \quad (2)$$

where λ is the relaxation rate.

The static field distribution width Δ obtained from the fits is presented in Fig. 4(a). In the paramagnetic state above 15 K, $\Delta = 0$, as expected from a fully dynamic field at the muon site. Below 15 K, Δ increases dramatically as the magnetic moments of Co^{II} and Fe^{III} freeze, generating a static field distribution. The size of this static field increases to $\Delta \sim 47$ MHz, corresponding to a width in field of ~ 3.5 kG at low temperatures. The dynamic relaxation rate, λ, exhibits a sharp increase below 20 K, peaks at $\sim$ 12.5 K and decreases slowly upon further cooling (Fig. 4(b)). The temperature dependence of λ is indicative of a sharp magnetic ordering phase transition at $T_c \sim 12.5$ K, where the increase as T approaches T_c from above is due to critical slowing down of the fluctuations. The relaxation at low temperatures is attributed to remnant local field fluctuations due to spin wave excitations [18]. Both λ and Δ temperature dependencies are in agreement with the ferrimagnetic behavior seen in the magnetization measurements.

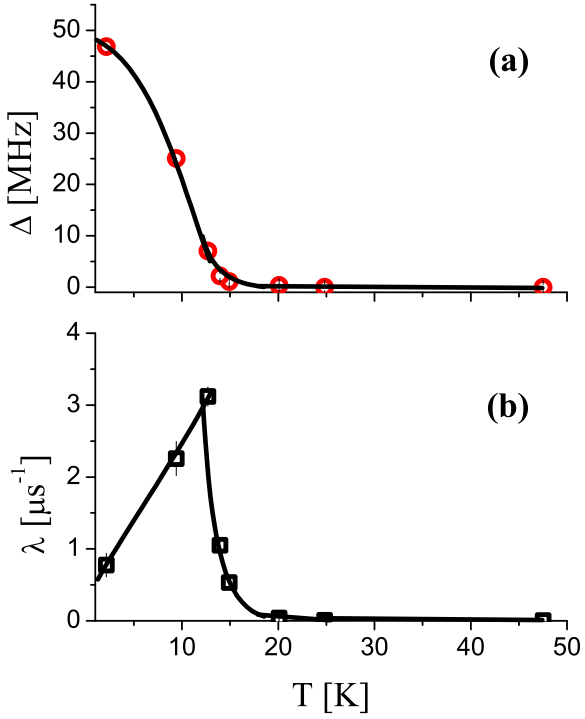

FIG. 4: The distribution of static fields (a) and the muon spin relaxation rate (b) in $Co_{1.5}$ as a function of temperature in an applied longitudinal field of 100 G. The solid lines are a guide for the eye.

Note that we find no missing fraction in low transverse fields in the paramagnetic phase, indicating no appreciable Muonium[2] formation. The absence of spontaneous

[2] Muonium (a μ^+e^- bound state) is known to react with CN [24].

spin precession in the magnetic phase in this nominally stoichiometric Co-Fe PBA and the square root relaxation behavior indicates that even here disorder, size and shape distribution of grain size and/or multiple inequivalent muon sites are sufficient to give a broad field distribution. In contrast, if $\gamma B_s \gg \Delta$ one expects muon spin precession at frequency γB_s. The magnitude of the typical field (measured by Δ) also gives an indication of the size of the fields that can be expected in the photomagnetic compositions, as well as their temperature dependencies. This behavior will be compared to that observed in the photomagnets $K_{0.2}Co_{1.4}$ and $Rb_{0.66}Co_{1.25}$.

D. Results in $K_{0.2}Co_{1.4}$: $x = 0.4$

We followed the procedure described in Ref. [9] to prepare the $K_{0.2}Co_{1.4}$ compound. Both the color and magnetization are in agreement with previous work [9]. $K_{0.2}Co_{1.4}$ is an example where red light changes the magnetization and the transition temperature [9, 12]. Similar

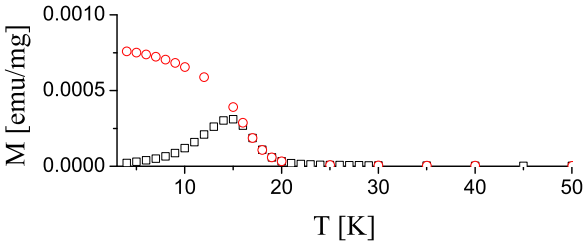

FIG. 5: The zero field (squares) and field (circles) cooled DC magnetization of $K_{0.2}Co_{1.4}$ measured at 100 G in a SQUID magnetometer.

to the $Co_{1.5}$, $K_{0.2}Co_{1.4}$ undergoes magnetic ordering below 20 K even in the unilluminated state. This is evident in the magnetization of $K_{0.2}Co_{1.4}$ which was measured in a SQUID magnetometer (see Fig. 5), and shows a dramatic increase at $T_c \sim 15$ K in both the FC and ZFC magnetization, in agreement with Ref. [9].

The muon relaxation in $K_{0.2}Co_{1.4}$ is similar to that found in $Co_{1.5}$ (see Fig. 6), where at low temperatures the muons experience a local field which is a combination of a static distribution of local fields and an additional small fluctuating component. However, the relaxation in this case is better described by a LKT multiplied by a square root exponential function,

$$A(t) = A_{\rm LKT}(t)e^{-\sqrt{\lambda t}}. \quad (3)$$

A Lorentzian static field distribution is typical in dilute spin glass systems where the breadth of the distribution is due to the distribution of muon sites with varying distances from the magnetic moments [23].

The temperature dependencies of the fit parameters Δ and λ in $K_{0.2}Co_{1.4}$ are similar to those seen in $Co_{1.5}$.

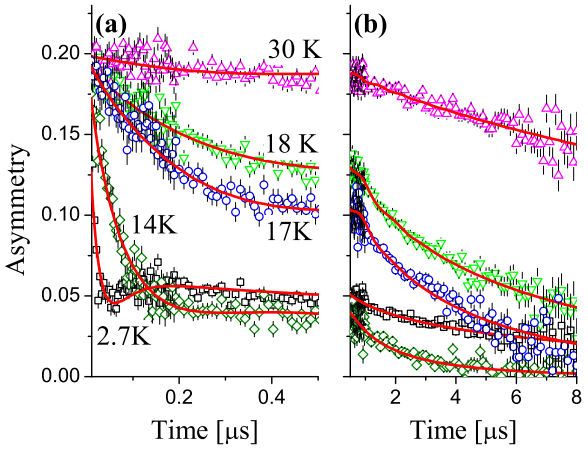

FIG. 6: (Color online) The muon spin relaxation as a function of time measured in $K_{0.2}Co_{1.4}$ at 100 G longitudinal field for different temperatures at (a) early and (b) long times. The solid lines are fits to the function described in the text

The distribution of static fields Δ, presented in Fig. 7(a), is zero above 15 K, indicating the muon spin relaxation is due entirely to a fluctuating field. Below this temperature Δ increases and saturates at low temperatures, where $\Delta = 33$ MHz corresponding to a width in field of ~ 2.5 kG, slightly smaller than that found in $Co_{1.5}$, as expected from a system with lower moment concentration. The relaxation rate λ, presented in Fig. 7(b), has a sharp increase below 20 K, peaks at $T \sim 12.5$ K, indicative of the slowing down of magnetic field fluctuations, and decreases slowly at lower temperatures. As expected the relaxation rate in $K_{0.2}Co_{1.4}$ is also lower than in $Co_{1.5}$, consistent with the smaller average local field experienced by muons in $K_{0.2}Co_{1.4}$.

E. Results in $Rb_{0.66}Co_{1.25}$: $x \simeq 0.17$

The compound $Rb_{0.66}Co_{1.25}$ was prepared according to the procedure described in Ref.[13]. The color, magnetization and the IR frequencies of CN stretching mode of the compound are in agreement with previous work [13]. The magnetization as a function of temperature at 100 G is featureless and very small compared to that in $Co_{1.5}$ and $K_{0.2}Co_{1.4}$ due to the high concentration of diamagnetic centers $Fe^{II}(t_{2g}^6, S = 0)$-CN-$Co^{III}(t_{2g}^6, S = 0)$. As can be seen in Fig. 8, the inverse susceptibility $(1/\chi)$ exhibits an almost linear[3] dependence on temperature,

[3] Note that the value of the magnetization for this paramagnetic compound is rather low, therefore the small deviation from the perfect linear behavior may be due to small inaccuracies in the measurements.

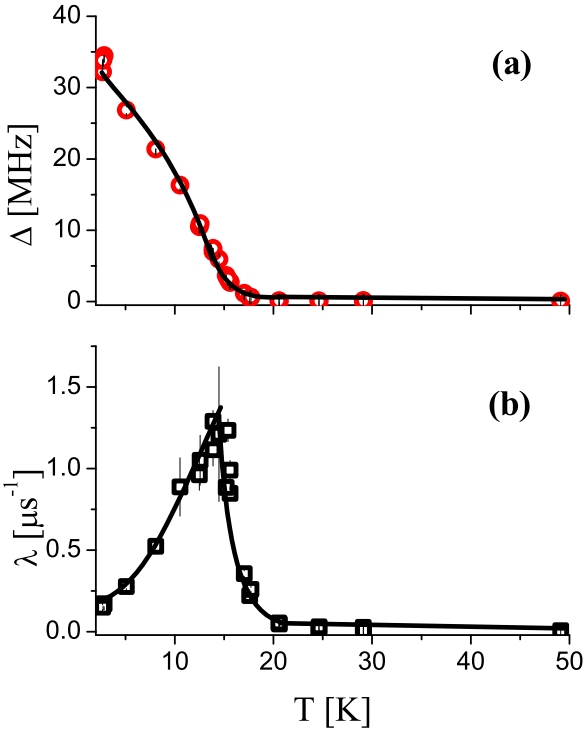

FIG. 7: The distribution of static fields (a) and muon spin relaxation rate (b) in $K_{0.2}Co_{1.4}$ as a function of temperature in a longitudinal field of 100 G. The solid lines are a guide for the eye.

indicating that unilluminated $Rb_{0.66}Co_{1.25}$ remains paramagnetic down to at least 4 K. In contrast to $Co_{1.5}$, para-

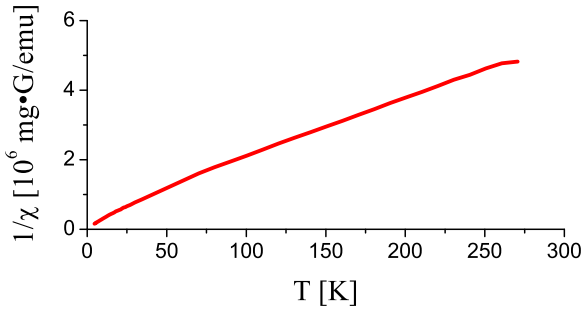

FIG. 8: The inverse susceptibility of $Rb_{0.66}Co_{1.25}$ as a function of temperature measured at 100 G.

magnetic $Rb_{0.66}Co_{1.25}$, is expected to show a strong response to visible light [13, 25].

The muon spin relaxation was measured in non-stoichiometric $Rb_{0.66}Co_{1.25}$ at different longitudinal fields and temperatures between 300 K and 2.3 K. The asymmetry at low LF (B = 40 G) and various temperatures is shown in Fig. 9. At this field the relaxation is slow at high temperatures and increases monotonically at low temperatures. In contrast, at high LF (B = 2.4 kG)

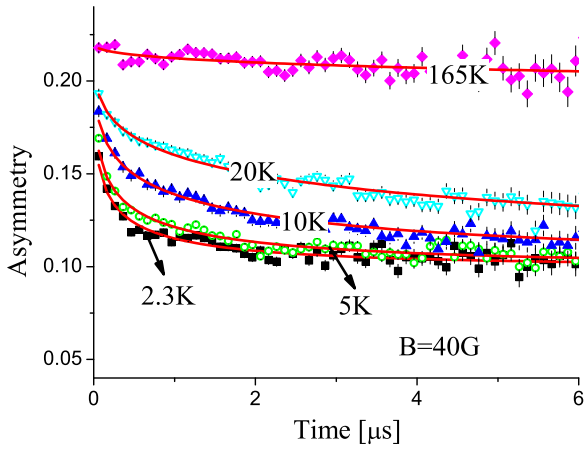

FIG. 9: (Color online) The muon spin relaxation in $Rb_{0.66}Co_{1.25}$ at LF B = 40 G and different temperatures.

the relaxation increases as the temperature is decreased, peaks at $T \sim 10$ K and then decreases at lower temperatures (see Fig. 10). Note the asymmetry measured in

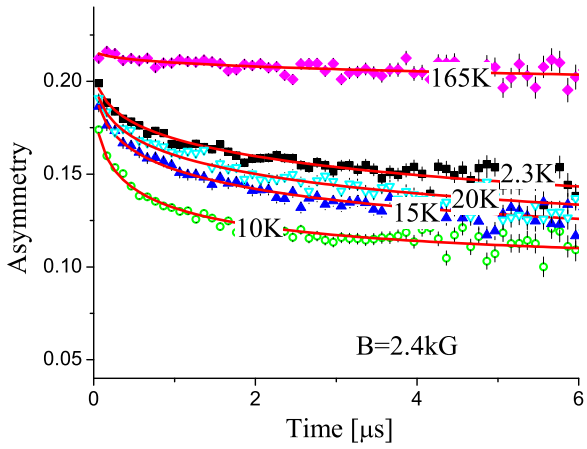

FIG. 10: (Color online) The muon spin relaxation in $Rb_{0.66}Co_{1.25}$ at B = 2.4 kG and different temperatures.

$Rb_{0.66}Co_{1.25}$ shows no dip/recovery at early times, indicating that the muons do not experience a static field component in this compound, and that the spin relaxation here is entirely dynamic in origin.

All spectra were fit with the sum of a stretched exponential and a non-relaxing background,

$$A(t) = A_0 \exp\left(-(\lambda t)^{0.35}\right) + Bg. \quad (4)$$

The background asymmetry, $Bg = 0.1$, is quite large and is due to muons missing the sample (9 mm diameter) and

stopping in the silver mask around it. In contrast, the other samples were large (15 mm diameter) and had little or no background, as is evident in Fig. 3(b) and 6(b). The relaxation rate λ is the average spin lattice relaxation (SLR) rate. The small value of the exponent 0.35 characterizing the distribution of relaxation rates is typical in dilute spin glass systems [23], suggesting a similar distribution of magnetic moments in $Rb_{0.66}Co_{1.25}$.

The average relaxation rate for all temperatures and fields investigated is presented in Fig. 11. Above 20 K the relaxation rate is field independent. However, below this temperature λ depends strongly on field and increases significantly as the temperature is lowered. At

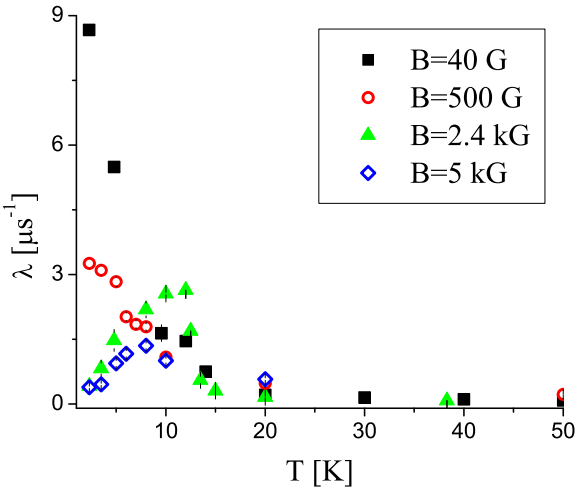

FIG. 11: (Color online) The muon spin relaxation rate in $Rb_{0.66}Co_{1.25}$ as a function of temperature at different longitudinal fields.

low fields ($40 - 1000$ G) the relaxation rate does not exhibit a peak, while at fields greater than 2.4 kG the relaxation rate peaks and then decreases at lower temperatures. This type of behavior is characteristic of magnetic cluster freezing seen in other molecular magnetic materials [5, 6, 7, 26, 27, 28]. Molecular magnets consist of clusters of magnetic ions with a large exchange coupling J between them, while a very weak dipolar coupling exists between neighboring molecules, such that at low temperatures they behave as non-interacting large magnetic moments ($\mathbf{m}$). In these systems a large increase in the relaxation rate is observed at low LF ($\mathbf{m} \cdot \mathbf{B} \ll J$) when the temperature is comparable to J. This increase is due to slowing down of the local field fluctuations at the muon site as the clusters coalesce. However, at high LF ($\mathbf{m} \cdot \mathbf{B} \gg J$) and low temperature the relaxation rate decreases as fluctuations in the molecular moments are quenched by the applied field, i.e. as the thermal energy becomes smaller than the molecular Zeeman splitting $k_B T < \mathbf{m} \cdot \mathbf{B}$.

These results strongly disagree with the conclusion, based on magnetization measurements similar to those of Fig.8, that $Rb_{0.66}Co_{1.25}$ remains a simple paramagnet down to low temperature [13]. Our μSR measurements show that even in the unilluminated ground state, a disordered magnetic state is forming below 20 K that is not apparent in the macroscopic magnetization.

The time-scale and size of the dynamics of the local field at the muon site can be estimated from the dependence of the muons' SLR on the applied LF at low temperature. In the fast fluctuation limit the SLR time follows [5, 29, 30]

$$T_1(B) = \alpha + \beta B^2, \tag{5a}$$

$$\alpha = \frac{1}{\Delta^2 \tau}, \tag{5b}$$

$$\beta = \frac{(2\pi\gamma)^2 \tau}{\Delta^2}. \tag{5c}$$

The correlation time (τ) and mean square of the transverse field distribution at the muon site in frequency units (Δ^2) are defined by the auto-correlation function of the local transverse field,

$$\gamma^2 \langle \mathbf{B}_\perp(t) \mathbf{B}_\perp(0) \rangle = \Delta^2 \exp(-t/\tau). \tag{6}$$

The fast fluctuation limit is defined by $\tau\Delta < 1$ [31]. Note that in Eq.5 and 6 an exponential spin relaxation function is assumed. However, the muons can occupy magnetically inequivalent sites in the lattice, and therefore experience a distribution of Δ values. As a result the spin relaxation becomes non-exponential (e.g. Eq. 4) and one should average over all possible values of Δ [5]. The linear relation in Eq. 5 still holds in this case, but Δ is interpreted as the average value of the local field distribution widths for all possible sites.

In Fig. 12 we plot the SLR time, $T_1 \equiv 1/\lambda$, at $T = 2.3$ K as a function of the applied magnetic field squared, B^2. We find that, as expected from Eq. 5, the relaxation time is proportional to B^2. The correlation time τ and the size of the local magnetic field calculated from the free constant $\alpha = 0.1147(9)$ μs and the slope $\beta = 0.401(1)$ μs/kG^2 of the linear relation [5], are $\Delta = 19.93(5)$ MHz and $\tau = 21.9(1)$ ns, justifying the assumption that we are in the fast fluctuation limit. Δ corresponds to a width in field of 0.587(2) kG, much smaller than that measured in $Co_{1.5}$ and $K_{0.2}Co_{1.4}$, and consistent with the smaller concentration of magnetic moments in $Rb_{0.66}Co_{1.25}$.

F. Sample Illumination

We attempted to observe photoinduced changes in the magnetism of $K_{0.2}Co_{1.4}$ and $Rb_{0.66}Co_{1.25}$ in a range of different configurations of sample mounting and optical illumination as discussed in section B. In other measurements [9, 12, 13, 17], similar light intensity was found to be sufficient to observe the photoinduced effect in both

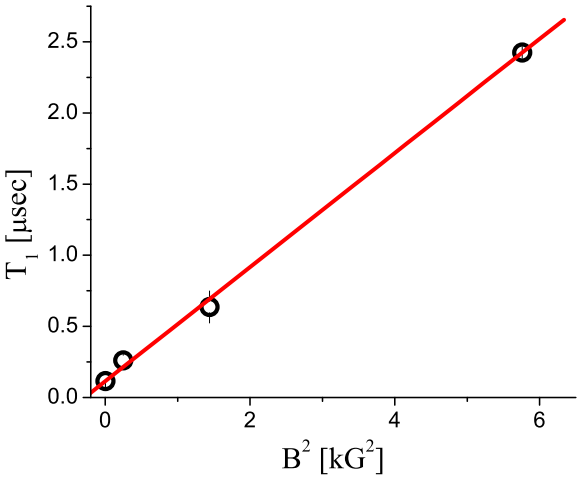

FIG. 12: The muon spin relaxation time at $T = 2.3$ K as a function of the magnetic field squared. The solid line is a linear fit $T_1 = \alpha + \beta B^2$ with $\alpha = 0.1147(9)$ μs and $\beta = 0.401(1)$ μs/kG^2.

compounds. However, in neither back nor front illumination configurations, even for illumination times up to ~ 5 hours at $T = 5$ K, did we observe a significant effect of the light on the μSR signals in $K_{0.2}Co_{1.4}$ or $Rb_{0.66}Co_{1.25}$. Heating effects of illumination were apparent in the sample thermometry, but were at most a few degrees. This is still well below the thermal reversion of the metastable state above ~ 100 K [13].

The lack of a photomagnetic effect in our data is probably the result of a mismatch between the stopping range of muons and the absorption length of light. Co-Fe PBAs are highly colored materials, but are also very opaque, a consequence of low energy *d-d* and metal-ligand charge transfer excitations. It has been shown that with the formation of the metastable magnetic centers, the material becomes less absorbing in the wavelength region relevant to the photomagnetism [32], thus it is possible that the photomagnetic state would eventually grow out from the illuminated surfaces, but such an effect was apparently not sufficient to influence the magnetism on the ~ 100 μm surface muon stopping range. A more favorable situation to study these effects is in a thin film geometry [33] using low energy muons [34] or β-NMR probes [35, 36, 37].

G. Summary and Conclusions

The close similarity of the temperature dependencies of Δ and λ in $Co_{1.5}$ and $K_{0.2}Co_{1.4}$ are strong indications that both compounds undergo similar magnetic transitions, from dynamic paramagnetism to long range magnetic order. However, in $Rb_{0.66}Co_{1.25}$ there is no evidence of freezing of the magnetic moments. We now present these results within the context of a simple site percolation model [15]. Assuming that the fraction of magnetic (Fe^{III} and Co^{II}) to non-magnetic (vacancies) centers in the system is p, the percolation theory predicts that above a critical value $p_c = 0.3116$ [15, 16] magnetic long range order is possible. In our compounds the number of non-magnetic centers is $1-2x$, therefore $p \equiv 2x$. In particular $p = 1, 0.8$ and ~ 0.34 for $Co_{1.5}$, $K_{0.2}Co_{1.4}$ and $Rb_{0.66}Co_{1.25}$, respectively. Note that p is well above the critical value for both $Co_{1.5}$ and $K_{0.2}Co_{1.4}$, and consequently long range magnetic order is expected, while for the $Rb_{0.66}Co_{1.25}$ compound p is close to the critical value, and therefore the system may not be able to achieve such order. Indeed, our results are consistent with long range magnetic order formed at low temperature in $Co_{1.5}$ and $K_{0.2}Co_{1.4}$, but not in $Rb_{0.66}Co_{1.25}$.

Compound	p	Δ [MHz]	Δ [kG]
$Co_{1.5}$	1.0	46.8 ± 1.2	3.45 ± 0.09
$K_{0.2}Co_{1.4}$	0.8	33.3 ± 1.0	2.46 ± 0.07
$Rb_{0.66}Co_{1.25}$	0.34	19.93 ± 0.05	0.587 ± 0.002

TABLE I: Summary of the average value of local field at the muon site, measured at $T \sim 2.3$ K.

The size of local magnetic field at low temperature is summarized in Table I. Although estimated from different muon relaxation behavior in the three compounds, Δ can be used as an estimate of the size of the local field, which clearly decreases with decreasing p as expected for a lower concentration of magnetic centers and a smaller average magnetic cluster size.

As Figs. 4, 7, and 11 demonstrate, the common energy scale that appears in all three compounds is $T \sim 12.5$ K. This corresponds to the measured strength of the superexchange coupling $J = 15$ K between neighboring Fe^{III} and Co^{II} in $Co_{1.5}$ [13]. Since the chemical structure and the CN bond length away from vacancies is identical in $Co_{1.5}$, $K_{0.2}Co_{1.4}$ and $Rb_{0.66}Co_{1.25}$, the coupling between Fe^{III} and Co^{II} pairs is expected to be very similar in all three compounds. Therefore, in the unilluminated state J is independent of the alkali metal M concentration $1 - p$. Note however, that this is not necessarily true near vacancies, and therefore after illumination the coupling between Fe^{III} and Co^{II} pairs may be different.

These results indicate that the magnetic properties of the Co-Fe PBAs in the unilluminated state depend strongly on the concentration of vacancies. We find evidence for long range order when the concentration of magnetic centers is above the critical value, p_c, as is the case in $Co_{1.5}$ and $K_{0.2}Co_{1.4}$, while near p_c we find evidence of magnetic cluster formation without freezing, in agreement with a simple site percolation model.

Acknowledgments

We thank N.D. Draper and D.B. Leznoff of Simon Fraser University for advice with the sample preparations, R.F. Kiefl for useful discussions, and B. Hitti and R. Abasalti for technical assistance with the measurements. This work was funded by TRIUMF and NSERC of Canada.

[1] A. N. Holden, B. T. Matthias, P. W. Anderson, and H. W. Lewis, Phys. Rev. **102**, 1463 (1956).
[2] R. M. Bozorth, ibid **103**, 572 (1956).
[3] F. Herren, P. Fischer, A. Ludi, and W. Halg, Inorg. Chem. **19**, 956 (1980).
[4] A. P. Ginsberg, Inorg. Chem. Acta, Reviews p. 45 (1971).
[5] Z. Salman, A. Keren, P. Mendels, V. Marvaud, A. Scuiller, M. Verdaguer, J. S. Lord, and C. Baines, Phys. Rev. B **65**, 132403 (2002).
[6] Z. Salman, A. Keren, P. Mendels, A. Scuiller, and M. Verdaguer, Physica B **106**, 289 (2000).
[7] T. Jestadt, M. Kurmoo, S. J. Blundell, F. L. Pratt, C. J. Kepert, K. Prassides, B. W. Lovett, I. M. Marshall, A. Husmann, K. H. Chow, R. M. Valladares, C. M. Brown, and A. Lappas, J. Phys.: Cond. Matt. **13**, 2263 (2001).
[8] K. Itoh and M. Kinoshita, eds., *Molecular magnetism: new magnetic materials* (Kodansha, Tokyo, 2000).
[9] O. Sato, T. Iyoda, A. Fujishima, and K. Hashimoto, Science **272**, 704 (1996).
[10] D. A. Pejakovič, J. L. Manson, J. S. Miller, and A. J. Epstein, J. Appl. Phys. **87**, 6028 (2000).
[11] N. Shimamoto, S. Ohkoshi, O. Sato, and K. Hashimoto, Inorg. Chem. **41**, 678 (2002).
[12] D. A. Pejakovič, J. L. Manson, J. S. Miller, and A. J. Epstein, Synthetic Metals **122**, 529 (2001).
[13] O. Sato, Y. Einaga, A. Fujishima, and K. Hashimoto, Inorg. Chem. **38**, 4405 (1999).
[14] T. Kawamoto, Y. Asai, and S. Abe, Phys. Rev. Lett. **86**, 348 (2001).
[15] D. Stauffer and A. Aharony, *Introduction to Percolation Theory* (London: Taylor and Francis, 1991).
[16] J. M. Paniagua, E. Alonso, L. M. del Rio, A. Jimenez, and A. Baeza, Eur. J. Phys. **18**, 182 (1997).
[17] D. A. Pejakovič, J. L. Manson, J. S. Miller, and A. J. Epstein, Phys. Rev. Lett. **85**, 1994 (2000).
[18] G. M. Kalvius, D. R. Noakes, and O. Hartmann, in *Handbook on the Physics and Chemistry of Rare Earths*, edited by G. Lander, K. Gschneider, and L. Eyring (Elsevier, 2001), vol. 32, p. 55.
[19] S. L. Lee, S. H. Kilcoyne, and R. Cywinski, *Muon Science* (SUSSP and Institute of Physics Publishing, 1998).
[20] K. H. Chow, B. Hitti, and R. F. Kiefl, in *Semiconductors and Semimetals*, edited by M. Stavola (Academic Press, New York, 1998), vol. 51A, p. 137.
[21] K. H. Chow, P. A. Pattenden, S. J. Blundell, W. Hayes, F. L. Pratt, T. Jestadt, M. A. Green, J. E. Millburn, M. J. Rosseinsky, B. Hitti, S. R. Dunsiger, R. F. Kiefl, C. Chen, and A. J. S. Chowdhury, Phys. Rev. B **53**, R14725 (1996).
[22] T. Jestadt, K. H. Chow, S. J. Blundell, W. Hayes, F. L. Pratt, B. W. Lovett, M. A. Green, J. E. Millburn, and M. J. Rosseinsky, Phys. Rev. B **59**, 3775 (1999).
[23] Y. J. Uemura, in *Muon Science: Muons in Physics, Chemistry and Materials*, edited by S. Lee, S. Kilcoyne, and R. Cywinski (SUSSP and Institute of Physics Publishing, 1998), chap. 4.
[24] J. M. Stadlbauer, B. W. Ng, Y. C. Jean, and D. C. Walker, J. Phys. Chem. **87**, 841 (1983).
[25] A. Goujon, F. Varret, V. Escax, A. Bleuzen, and M. Verdaguer, Polyhedron **20**, 1347 (2001).
[26] A. Lascialfari, Z. H. Jang, F. Borsa, P. Carretta, and D. Gatteschi, Phys. Rev. Lett. **81**, 3773 (1998).
[27] S. J. Blundell, F. L. Pratt, T. Lancaster, I. M. Marshall, C. A. Steer, S. L. Heath, J. F. Letard, T. Sugano, D. Mihailovic, and A. Omerzu, Polyhedron **22**, 1973 (2003).
[28] S. J. Blundell and F. L. Pratt, J. Phys. Cond. Mat. **16**, R771 (2004).
[29] Y. J. Uemura, T. Yamazaki, D. R. Harshman, M. Senba, and E. J. Ansaldo, Phys. Rev. B **31**, 546 (1985).
[30] A. Keren, Phys. Rev. B **50**, 10039 (1994).
[31] A. Keren, Ph.D. thesis, Columbia University (1994).
[32] O. Sato, S. Hayamai, Y. Einaga, and Z. Gu, Bull. Chem. Soc. Jpn. **76**, 443 (2002).
[33] J.-H. Park, Y. D. Huh, E. Čižmár, S. G. Gamble, D. R. Talham, and M. W. Meisel, J. Mag. Magn. Mater. **272**, 1116 (2004).
[34] P. Bakule and E. Morenzoni, Cont. Phys. **45**, 203 (2004).
[35] G. D. Morris, W. A. MacFarlane, K. H. Chow, Z. Salman, D. J. Arseneau, S. Daviel, A. Hatakeyama, S. R. Kreitzman, C. D. P. Levy, R. Poutissou, R. H. Heffner, J. E. Elenewski, L. H. Greene, and R. F. Kiefl, Phys. Rev. Lett. **93**, 157601 (2004).
[36] Z. Salman, E. P. Reynard, W. A. MacFarlane, K. H. Chow, J. Chakhalian, S. R. Kreitzman, S. Daviel, C. D. P. Levy, R. Poutissou, and R. F. Kiefl, Phys. Rev. B **70**, 104404 (2004).
[37] Z. Salman, R. F. Kiefl, K. H. Chow, M. D. Hossain, T. A. Keeler, S. R. Kreitzman, C. D. P. Levy, R. I. Miller, T. J. Parolin, H. Saadaoui, J. D. Schultz, M. Smadella, D. Wang, and W. A. MacFarlane, Submitted.